Carbohydrate Polymers 152 (2016) 222–230

Contents lists available at ScienceDirect

Carbohydrate Polymers

journal homepage: www.elsevier.com/locate/carbpol

Structure and bioactivity of a polysaccharide containing uronic acid from *Polyporus umbellatus* sclerotia

Pengfei He[a,b], Anqiang Zhang[b,c,*], Fuming Zhang[c], Robert J. Linhardt[c,d], Peilong Sun[b,*]

[a] College of Biotechnology and Bioengineering, Zhejiang University of Technology, Hangzhou 310032, China
[b] College of Ocean, Zhejiang University of Technology, Hangzhou 310032, China
[c] Departments of Chemistry and Chemical Biology and Biomedical Engineering, Center for Biotechnology and Interdisciplinary Studies, Rensselaer Polytechnic Institute, Troy, NY 12180, USA
[d] Department of Biological Science, Center for Biotechnology and Interdisciplinary Studies, Rensselaer Polytechnic Institute, Troy, NY 12180, USA

ARTICLE INFO

Article history:
Received 22 April 2016
Received in revised form 29 June 2016
Accepted 3 July 2016
Available online 4 July 2016

Keywords:
Polyporus umbellatus
Polysaccharide
Structure-function relationship
Nuclear magnetic resonance spectroscopy
Atomic force microscopy
Antioxidant activity

ABSTRACT

Polyporus umbellatus is a medicinal fungus, has been used in traditional Chinese medicine for thousands years for treatment of edema, scanty urine, vaginal discharge, jaundice and diarrhea. The structure of a soluble polysaccharide (named PUP80S1), purified from the sclerotia of *Polyporus umbellatus* was elucidated by gas chromatography (GC), GC–mass spectrometry and nuclear magnetic resonance spectroscopy. PUP80S1 is a branched polysaccharide containing approximately 8.5% uronic acid and having an average molecular weight of 8.8 kDa. Atomic force microscopy of PUP80S1 reveals a globular chain conformation in water. Antioxidant tests, Oxygen radical absorption capacity and 2,2-diphenyl-1-picrylhydrazyl radical scavenging assays indicate that PUP80S1 possesses significant antioxidant activity. But the related polysaccharide, PUP60S2, which contains more uronic acid residues and a higher level of branching, shows better antioxidant activity. These results suggest that structure features of polysaccharides play an important role in their physiological functions.

1. Introduction

In recent years, polysaccharides have attracted a great deal of attention from the medical and food industry as bioactive ingredients and food additives (Perez-Mendoza et al., 2015; Ruthes, Smiderle, & Iacomini, 2016). Besides their numerous biological activities, polysaccharides can also support other applications in regenerative therapies and as nano-sized drug-delivery systems (Forget et al., 2013; Mizrahy & Peer, 2012). The structural features of polysaccharides, including their molecular size, frequency of branching, monosaccharide composition, conformation, types and sequence of linkages, determine their physical and physiological properties (Ferreira, Passos, Madureira, Vilanova, & Coimbra, 2015; Jin, Zhao, Huang, Xu, & Shang, 2012). Hence, prior to their utilization for any pharmaceutical or nutraceutical application, it is essential to have a clear understanding of their structural features.

Polysaccharides extracted from natural sources are generally acknowledged to have a rather low toxicity leading to their consumption as functional foods (Prajapati, Maheriya, Jani, & Solanki, 2014). Medicinal fungi are an important source of bioactive polysaccharides. The various applications and structural features of the polysaccharides from medicinal fungi, such as *Ganoderma lucidum*, have been extensively described (Liao et al., 2013; Liu et al., 2014; Nie, Zhang, Li, & Xie, 2013).

Polyporus umbellatus (Pers.) Fries, also known as *Grifola umbellata* (Pers.) Pilát, have been widely used as a traditional Chinese medicine for over 2000 years. Their main medicinal part, the sclerotia, is widely utilized in Asia for treatments of edema, scanty urine, vaginal discharge, as well as jaundice and diarrhea (Bensky, Gamble, & Kaptchuk, 1993). Polysaccharides are acknowledged as dominant active ingredient in sclerotia of *P. umbellatus* and are endowed with various activities, including anticancer, hepatoprotective, immuno-enhancing, radioprotective and antioxidative activity (Li, Xu, & Chen, 2010; Lin & Wu, 1988; Peng et al., 2012; Ueno, Okamoto, Yamauchi, & Kato, 1982; Wu et al., 2011; Zhang et al., 2011). However, in stark contrast to these reported activities, there are few reports on their structural features, greatly limiting their practical application. In the current study, we examined the structural features of polysaccharides from the sclerotia of *P.*

* Corresponding authors at: College of Ocean, Zhejiang University of Technology, Hangzhou, 310032, China
E-mail addresses: zhanganqiang@zjut.edu.cn (A. Zhang), sun_pl@zjut.edu.cn (P. Sun).

http://dx.doi.org/10.1016/j.carbpol.2016.07.010
0144-8617/

umbellatus and to determine their structure-activity relationship. A water-soluble polysaccharide had been reported in our previous work (He et al., 2016). The aim of this study is to elucidate the structure and conformation of another novel polysaccharide, and to generate basic understanding of its structure–function relationship by evaluating the antioxidant activities of these two polysaccharides having similar structures.

2. Materials and methods

2.1. Materials

DEAE Sepharose fast flow, high-resolution Sephacryl S-100 and S-200 were purchased from GE Healthcare. T-series dextran standards, trifluoroacetic acid (TFA), dimethyl sulfoxide (DMSO) and monosaccharide standards (D-Gal, L-Fuc, L-Rha, D-Man, D-Xyl, D-Glc), 6-hydroxy-2,5,7,8-tetramethylchroman-2-carboxylic acid (Trolox) and ascorbic acid (Vitamin C, Vc) were from Sigma. All the other reagents were of analytical reagent grade and made in China.

2.2. Isolation and purification of polysaccharide

The extraction and purification were conducted according to the procedures as described in our previous study (He et al., 2016). Briefly, following soaking overnight with 95% alcohol to remove small ethanol extractable molecules, the dried ground sclerotia of *P. umbellatus* (500 g) was extracted three-times (2 h for each time) with boiling distilled water. All aqueous extracts were then pooled and concentrated under reduced pressure. Fractional precipitation was carried out by slowly adding alcohol into the concentrated aqueous extract to sequentially bring final alcohol concentration to 30, 60 and 80% (v/v). After ethanol precipitation, three fractions (30, 60 and 80% fraction) were obtained with yields of around 3.87, 5.82 and 5.38 g, respectively. A part of 80% fraction (3.5 g) was further purified by binding to a DEAE Sepharose column (26 mm × 100 cm) with step-wise salt elution. The fraction eluting with 0.1 M sodium chloride solution was combined and desalted using a Sephacryl S-100 column (16 mm × 100 cm) eluted with water, followed by further purification with Sephacryl S-200 column eluted with water. The main fraction was pooled, lyophilized, and designated as PUP80S1, which had a yield of 0.64 g.

2.3. Chemical determination of total sugar, protein and uronic acid in polysaccharide

Phenol-sulfuric acid method was employed to determine sugar content using glucose as reference (Dubois, Gilles, Hamilton, Rebers, & Smith, 1956). The content of uronic acid was determined by meta-hydroxydiphenyl assay of Blumenkrantz and Asboe-Hansen (1973) as modified by Filisetti-Cozzi and Carpita (1991) using sulfamate to eliminate the interference from neutral sugars, glucuronic acid was used as reference. Protein content was evaluated using an enhanced BCA protein assay kit (Beyotime Biotechnology, China).

2.4. Homogeneity and molecular weight

The homogeneity and molecular weight of PUPF80S1 was determined using high performance size-exclusion chromatography (HPSEC) on a Waters 2695 system equipped with a Waters 2414 refractive index detector. Sample was separated on a TSK-Gel PW_{XL} G4000 column eluted with 0.1 M aqueous $NaNO_3$ solution at a flow rate of 0.6 mL/min. The molecular weight of PUPF80S1 was estimated by reference to a calibration line derived from T-series dextrans with known molecular weight (5 kDa, 12 kDa, 80 kDa, 150 kDa, 270 kDa and 670 kDa).

2.5. FT-IR spectroscopy

Fourier-transformed infrared (FT–IR) spectra were recorded in the range of 4000–500 cm^{-1} on a Nicolet 6700 FT–IR spectrometer (Thermo, USA).

2.6. Reduction of carboxyl groups

The reduction of carboxyl groups in PUPF80S1 were carried out according to the method of Taylor and Conrad (1972). Briefly, about 20 mg of sample was dissolved in 10 mL water and then incubated with 1 mmol of 1-ethyl-3-(3-dimethylaminopropyl) carbodimide (EDC) for 2 h. The pH was kept at 4.75 with 0.1 M HCl using automatic titration during incubation. Reduction was thereafter carried out by slow addition of 2 M $NaBH_4$ solution using a hypodermic syringe. The reduction reaction proceeded at room temperature for 60 min during which 4 M HCl was used to keep the pH at 7.0 with automatic titration. After dialysis overnight against distilled water, the reduction procedure was conducted a second time to afford completely reduced PUP80S1, which was collected, dialyzed, lyophilized and designated as PUP80S1R. The complete reduction was confirmed by negative results in determination of uronic acid for PUP80S1R using meta-hydroxydiphenyl assay.

2.7. Monosaccharide compositional analysis

The monosaccharide composition was determined by gas chromatography (GC) after reduction and acetylation as reported by Wolfrom and Thompson (1963a, 1963b). Briefly, samples were hydrolyzed with TFA (2 M, 4 mL) at 110 °C for 2 h. Excess TFA was removed with methanol and the mixture was reduced through the addition of $NaBH_4$ solution. Acetylation was then conducted with acetic anhydride to give alditol acetates, which were determined by GC. GC was performed on an Agilent 7890N instrument coupled using an HP–5 capillary column (30 m × 0.32 mm × 0.25 μm) and a flame-ionization detector. The oven temperature was set as follows: increasing from 120 °C (1 min) to 240 °C at 10 °C/min and holding at 240 °C for 6.5 min. The temperatures of both injector and detector were set at 250 °C. Nitrogen was used as carrier gas. Monosaccharide standards were used to qualify the monosaccharide compositions.

2.8. Methylation analysis

Methylation analysis was carried out for determination of the linkage types between residues according to the method of Anumula and Taylor (1992). Briefly, polysaccharide sample (3 mg) was dissolved in DMSO (0.5 mL) and then methylated with addition of a fine suspension of NaOH in DMSO (0.6 mL) and methyl iodide (0.6 mL). After reaction termination with water, $CHCl_3$ was added to extract the resulting per-methylated products. For complete methylation this procedure was repeated again on the $CHCl_3$ extract after evaporation resulting in the disappearance of the hydroxyl absorption in IR spectrum. After successive hydrolysis with HCO_2H (88%, 3 mL) at 100 °C for 3 h and TFA (4 mL) at 110 °C for 6 h, the per-methylated polysaccharide was reduced and acetylated as described in monosaccharide analysis. The resulting partially methylated alditol acetates (PMAAs) were then determined by GC-mass spectrometry (MS). The oven temperature program was set as same as that used for GC analysis. The temperatures of both injector and detector were set at 250 °C. Helium was used as carrier gas.

2.9. Nuclear magnetic resonance (NMR) spectroscopy

Before being dissolved in D_2O (0.5 mL) for NMR analysis, PUPF80S1 was dried overnight in vacuum desiccator with P_2O_5 and deuterium exchanged by freeze-drying twice from D_2O. NMR spectra were record on a Bruker AVANCE III (500 MHz) NMR spectrometer including ^{1}H NMR (25 °C and 60 °C), ^{13}C NMR, ^{1}H–^{1}H correlation spectroscopy (COSY), total correlation spectroscopy (TOCSY), nuclear Overhauser enhancement spectroscopy (NOESY), heteronuclear single-quantum correlation (HSQC), heteronuclear multiple bond correlation (HMBC). HDO (25 °C, δ 4.78) was used as an internal reference for ^{1}H chemical shifts and 4,4-dimethyl-4-silapentane-1-sulfonic acid (DSS) was used as an internal standard set at δ 0.00 for the ^{13}C chemical shifts.

2.10. Atomic force microscopy (AFM)

PUP80S1 was dissolved in Milli-Q water to yield a stock solution of 1.0 mg/mL, which was stirred 2 h to achieve complete dissolution. The stock solution was gradually diluted to 0.1 μg/mL and stirred for 6 h while heating to 60 °C before deposition for AFM imaging. Sample aliquots of 20 μL were deposited on substrates (mica pre-treated with 2 M $NiCl_2$), left to adsorb for 30 s at room temperature, rinsed drop-wise with 1 mL Milli-Q water, and dried with pressurized air. The surface topology was scanned in dry-state on A Park XE-70 Atomic Force Microscope (AFM, Park Scientific Instruments, Korea). The AFM was operated in tapping mode under ambient conditions using commercial silicon nitride cantilevers.

2.11. Antioxidant activities assay

2.11.1. Oxygen radical absorption capacity (ORAC) assay

The ORAC assay was applied according to the method as described by Dávalos, Gómez-Cordovés and Bartolomé (2004). Briefly, the reaction was conducted in 75 mM sodium phosphate buffer (pH 7.4) at 37 °C with a final reaction mixture of 200 μL. Samples (20 μL) were pre-incubated with 120 μL of fluorescein (70 nM, final concentration) for 15 min. When 2,2′-azobis (2-amidinopropane) dihydrochloride FAAPH solution (60 μL; 12 mM, final concentration) was rapidly added, reaction mixtures were immediately subjected to fluorescence measurement (every two min for 98 min). The microplate was automatically shaken prior each reading. A blank with sodium phosphate buffer instead of samples and calibration solutions using Trolox were also conducted. The ORAC value was calculated from the net area under the fluorescence decay curve (AUC), which was obtained by subtracting the AUC corresponding to the blank. Final results were in μmol of Trolox equivalent/g of sample.

2.12. 1,1-Diphenyl-2-picryl-hydrazyl (DPPH) scavenging assay

The DPPH radical scavenging activity was tested according to previous studies (Hua, Zhang, Huang, Yi, & Yan, 2014) with a minor modification. Briefly, 2 mL of freshly prepared DPPH methanolic solution (0.2 mM) was mixed with 2 mL of various concentration samples (0.1-2.0 mg/mL) for 30 min at 37 °C in the dark. The absorbance was then measured at 517 nm. Ascorbic acid (Vc) was used as positive control. The scavenging effect was calculated using the following equation:

$$\text{Scavenging rate}(\%) = [1 - (A_i - A_j)/A_0] \times 100,$$

where A_0 is the absorbance with distilled water instead of sample, A_i is the absorbance of sample mixed with DPPH solution, and A_j is the absorbance of the sample without DPPH solution.

All data were expressed as means ± standard deviation from triplicate samples.

3. Results and discussion

3.1. Isolation, purification, and properties of PUP80S1

Following a series of purification performed on DEAE-anion exchange and gel-filtration chromatography, a water-soluble polysaccharide, PUP80S1, was prepared from sclerotia of *P. umbellatus*. Its homogeneity was evident from the elution of a single symmetrical peak in HPSEC chromatography (Fig. 1a). This sample showed 90.1% carbohydrate and 7.5% of protein. Furthermore, it was an acid polysaccharide containing about 8.5% uronic acid with a molecular weight of 8.8 kDa, based on reference to dextran calibration standards.

The FT-IR spectrum (Fig. 1b) of PUP80S1 revealed the characteristic absorption bands of polysaccharide. An intense and wide absorption band at 3399.9 cm^{-1} was attributed to the O—H stretching vibration. A band at 2923.6 cm^{-1} was assigned to the C—H stretching vibration. The bands observed in the region of 1000–1200 cm^{-1} belonged to the absorption of stretch vibration of C—O—C and C—O—H (Zhang et al., 2015). The peaks at 1376.9 cm^{-1} and 1319.1 cm^{-1} could be attributed to the bending vibration of C—H and twisting vibration of H—C—H, respectively (Venkatesan, Qian, Ryu, Ashok Kumar, & Kim, 2011). An additional two bands at 1640.0 cm^{-1} and 1413.6 cm^{-1}, respectively, were contributed by asymmetrical and symmetrical stretching vibration of COO^- (Nejatzadeh-Barandozi & Enferadi, 2012), which confirmed the presence of uronic acid.

3.2. Monosaccharide composition of PUP80S1

The GC elution profile for PUP80S1 revealed only one peak corresponding to glucose. Since acetates of uronic acids are unsuitable for GC analysis (Ruiz-Matute, Hernández-Hernández, Rodríguez-Sánchez, Sanz, & Martínez-Castro, 2011), the acidic sugar composition of PUP80S1 was analyzed by reduction of uronic acids into their corresponding hexoses. Also, only one peak was observed in GC chromatogram corresponding to glucose from the reduced PUP80S1R. These GC results of the polysaccharide consisted of glucose and glucuronic acid corresponding to the neutral and acid domains of PUP80S1.

3.3. Structural analysis of PUP80S1

Methylation analysis was a typical technique for elucidation of the types of glycosyl linkages and had been widely used in structure analysis of polysaccharides. GC–MS results (Table 1) of PMAAs derived from PUP80S1 gave five peaks, a 2,3,4,6-tetra-*O*-methyl-glucose, a 2,4,6-tri-*O*-methyl-glucose, a 2,3,6-tri-*O*-methyl-glucose, a 2,3,4-tri-*O*-methyl-glucose and a 2,4-di-*O*-methyl-glucose, which corresponded to terminal, 3-linked, 4-linked, 6-linked and 3,6-linked glucose residues. In addition, the reduced PUP80S1R was instead subjected to methylation analysis to obtain the information on acid residues. It produced the same five products as those derived from unreduced PUP80S1 (Table 1), indicating that no new linkage was formed after reduction. The different molar ratio between PUP80S1 and PUP80S1R in Table 1 are apparently caused by the presence of small amounts of uronic acids. Reduction of corresponding glucuronic acid seems to contribute to more 3-linked and 4-linked glucose for PUP80S1R. The presence of linkage of 3,6-linked indicates that PUP80S1 is a branched polysaccharide. The degree of branching (DB) was 22.8% based on the calculation method reported by Chen et al. (2015).

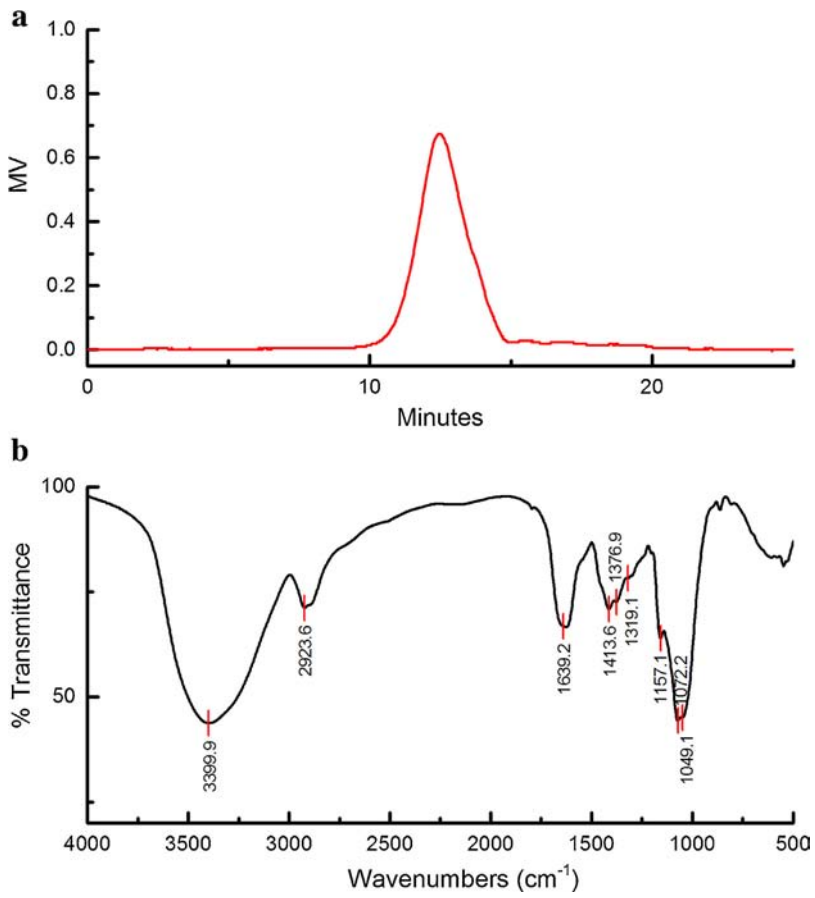

Fig. 1. The physicochemical properties of PUP80S1 from sclerotia of Polyporus umbellatus. (a): HPSEC chromatography eluted with 0.1 M NaCl; (b): FT–IR spectrum.

Table 1
Methylation analysis of PUP80S1 and its reduction product (PUP80S1R) using GC–MS.

Retention time (min)	Methylated sugars	Substituted sugar unit	Molar ratios [a]		Major mass fragments (*m*/*z*)
			PUP80S1	PUP80S1R	
9.61	2,3,4,6-Me_4-Glc	terminal-Glc*p*	1.16	1.05	43,71,87,101,117,129, 145, 161,205
10.56	2,4,6-Me_3-Glc	3-linked-Glc*p*	1.63	1.98	43,68,71,87,101,117, 129, 161,233
10.67	2,3,6-Me_3-Glc	4-linked-Glc*p*	0.82	1.12	43,71,87,101,113,117, 129,161,233
10.89	2,3,4-Me_3-Glc	6-linked-Glc*p*	4.11	3.95	43,87,99,101,117,129, 161,189,233
11.79	2,4-Me_2-Glc	3,6-linked-Glc*p*	1.00	1.00	43,87,117,129,139,159, 175,189,233

[a] Molar ratio was calculated from peak areas.

The exact structures and substituents of these components were further established and confirmed by NMR spectroscopy. ^{1}H NMR spectrum revealed two groups of anomeric protons at δ 4.47–4.57 and δ 4.69–4.80 in the anomeric region between δ 4.30 and 5.90, as well as other non-anomeric protons in the region of δ 3.20–4.25. Correspondingly, all anomeric carbon signals overlapped at around δ 102.90 and non-anomeric carbons fell in the region of δ 60.00–86.00. Two negative signals at δ 60.70 and δ 68.70 in DEPT-135 spectrum, arising from methylene of hexoses, were indicative of the presence of both an unsubstituted and substituted C6 position. Although signals of uronic acid were too weak to be distinguishable from noise, two signals at δ 175.00 and 175.25 ppm, clearly observed in HMBC, corroborated the presence of the uronic acids. Severe overlap of resonance signals made it difficult to directly obtain number of residues from their anomeric signals. But seven carbohydrate residues could be easily found from COSY spectrum (Fig. 2a), which were designated as A-G in an ascending sequence of anomeric protons chemical shifts.

The chemical shifts of all protons were completely assigned by trace resonance in COSY spectrum in sequence, starting from H1, as shown in Fig. 2a. These assignments were checked using TOCSY and NOESY spectra. Most corresponding carbons were assigned by HSQC spectrum (Fig. 2b), except for C6 of residue B and F, which were respectively identified from correlations at δ 3.76/175.25 and δ 3.87/175.00 in the HMBC spectrum. These carbonyl signals revealed that residue B and F were acid residues. All chemical shifts are summarized in Table 2. These residues were identified after complete assignments of chemical shifts. Arising from transfer of magnetization of H1 to H5 observed in TOCSY spectrum, all residues were assigned to *gluco*-configuration (Gheysen, Mihai, Conrath, & Martins, 2008). Anomeric protons in the region of δ 4.4–4.8 were indicative of the β-anomeric configuration (Yin, Lin, Nie, Cui, & Xie, 2012). The linkage positions of the residues were readily identified by the downfield shift of the signals of the linkage carbons. Comparison with chemical shifts of reference analogous compounds suggested that residue A-G were →6)-β-D-Glc*p*-(1→, →3)-β-D-Glc*p*A-(1→, →3)-β-D-Glc*p*-

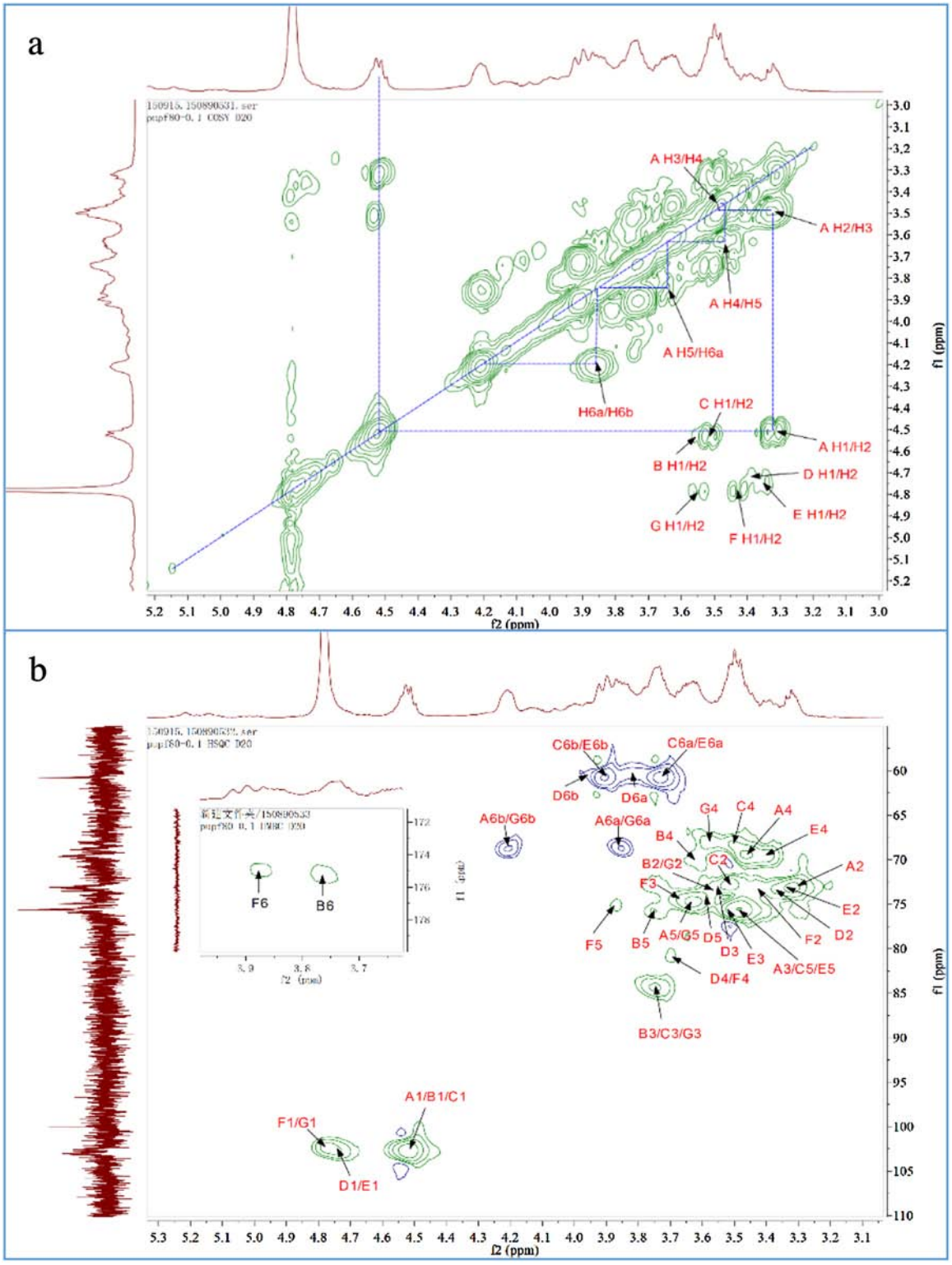

Fig. 2. 1D NMR spectra of PUP80S1 recorded in D_2O at 25 °C. (a): COSY spectrum, the dash line showed the procedures for the assignments of protons of A starting from H1; (b): HSQC spectrum, inset image was parts of HMBC spectrum for determination of C6 of B and F. A-G were seven residues of PUP80S1 in an ascending sequence of anomeric protons chemical shifts.

(1→, →4)-β-D-Glc*p*-(1→, β-D-Glc*p*-(1→, →4)-β-D-Glc*p*A-(1→ and →3,6)-β-D-Glc*p*-(1→, respectively. These results agree with those of the methylation analysis when the reduction of uronic acid to its corresponding hexose residue is taken into consideration for PUP80S1R.

NOESY and HMBC experiments were carried out to determine the sequence of these hexose residues. The cross-peak δ 4.51/3.86 in NOESY spectrum revealed that H1 of residue A showed strong inter-residual NOE correlation to H6a of residue A or residue G. This implied residue A was joined to *O*-6 of residue A or residue G. Residue B (or residue C) was joined to *O*-6 of residue A and *O*-4 of

Table 2
^{1}H and ^{13}C chemical shift data (ppm) data of PUP80S1.

Residues	Chemical shifts (δ)					
	H1/C1	H2/C2	H3/C3	H4/C4	H5/C5	H6a, 6b/C6
A	4.51	3.32	3.49	3.47	3.63	3.86, 4.21
→6)-β-D-Glc*p*-(1→	102.88	73.05	75.54	69.45	74.73	68.70
B	4.525	3.56	3.75	3.62	3.76	
→3)-β-D-Glc*p*A-(1→	102.88	73.05	84.28	69.94	75.74	175.25
C	4.533	3.52	3.74	3.50	3.48	3.73, 3.91
→3)-β-D-Glc*p*-(1→	102.88	72.78	84.51	68.46	75.54	60.71
D	4.72	3.38	3.54	3.70	3.61	3.81, 3.96
→4)-β-D-Glc*p*-(1→	102.82	73.28	73.14	80.89	74.25	60.50
E	4.74	3.36	3.52	3.41	3.49	3.73, 3.91
β-D-Glc*p*-(1→	102.80	73.27	75.54	69.45	75.54	60.71
F	4.78	3.43	3.67	3.70	3.87	
→4)-β-D-Glc*p*A-(1→	102.46	73.15	74.60	80.89	75.23	175.00
G	4.78	3.55	3.76	3.58	3.65	3.86, 4.21
→3,6)-β-D-Glc*p*-(1→	102.46	72.93	84.04	68.25	74.67	68.70

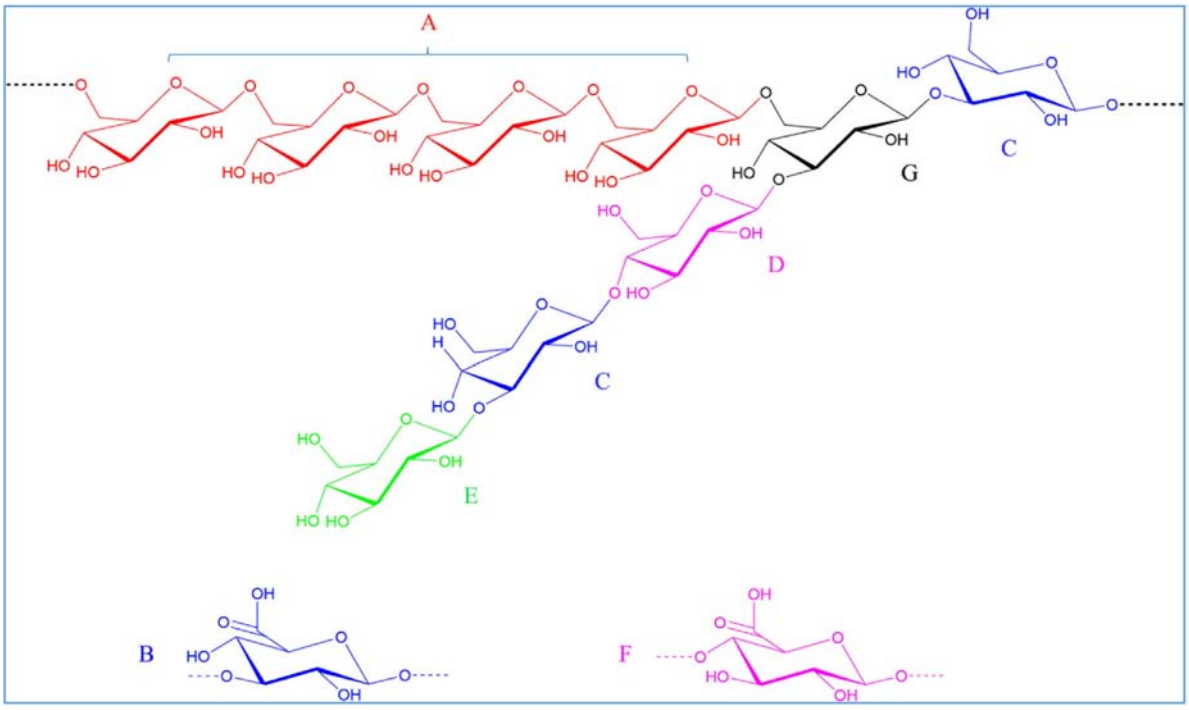

Fig. 3. Proposed structure of PUP80S1 from sclerotia of *Polyporus umbellatus*, where C and D may be occasionally displaced by their corresponding uronic acids B and F.

residue D (or F) evident from cross-peaks δ 4.53/3.86 (H6a of residue A) and δ 4.53/3.70 (H4 of residue D/F), respectively. Cross-peaks δ 4.72/3.76 and δ 4.78/3.76, respectively arising from inter-residual NOE correlations from H1 of residue D and residue F to H3 of residue G, indicated both residue D and F were joined to *O*-3 of residue G. Both residue E and G were linked to *O*-3 of residue B (or residue C) due to NOE correlations (δ 4.74/3.74 and δ 4.78/3.74) between their H1 and H3 of residue B (or residue C). These linkages sequence were also corroborated by the long-range correlations observed between H1 of residue A and C6 of residue A or G, H1 of residue B (or C) and C6 of residue A, H1 of residue D (and F) and C3 of residue G, H1 of residue E and C3 of residue B (or C), 1H of residue G and C3 of residue B (or C).

Based on the sugar composition, methylation analysis and NMR spectroscopy, the structure that better summarizes chemical and spectroscopical data of PUP80S1 is proposed in Fig. 3.

To our best knowledge, this structure is unique although β-glucans with similar structures have been reported for other fungi. A polysaccharide called HBP, extracted from the fruiting bodies of *Sarcodon pratus*, possessed a β-(1→6)-D-glucan backbone substituted at *O*-3 by tetrasaccharide side chains, whereas it had a lower degree of branching (DB) of 14.5% and no β-(1→3)-D-Glc*p* in its backbone (Han, Chai, Jia, Han, & Tu, 2010). A β-glucan extracted from fruiting bodies of *P. umbellatus*, *Zhuling* polysaccharide, presented a mixed 1 → 6, 1 → 4-linked backbone with trisaccharide side chains jointed to *O*-3 of β-(1→6)-D-Glc*p* and about 44.5% of DB values (Dai et al., 2012). However, PUP80S1 has a structure with a mixed 1 → 6, 1 → 3-linked backbone and DB around 22.8%. Additionally, a small percentage of uronic acid was present in PUP80S1, which has rarely been reported in similar β-glucans.

PUP80S1 was also different from polysaccharides previously reported for the sclerotia of *P. umbellatus*, although similar compositions may have been reported. Ueno, Abe, Yamauchi and Kato (1980) reported an alkali-soluble glucan having linkages of terminal, 3-linked and 3,6-linked, but no 4-linked and 6-linked glucose. A similar, but different polysaccharide, PUP60S2, was also described in our previous study (He et al., 2016). PUP60S2 contained fewer β-(1→6) and β-(1→3) linkages in its repeating blocks, a greater

Table 3
The results of antioxidant activity assay of PUP80S1 and PUP60S2.

Sample	ORAC (μmol TE/g)[a]	DPPH		
		Concentration (mg/mL)	Scavenging ratio (%)	IC50 (mg/mL)
PUP60S2	958.32 ± 26.05[b]	0.1	10.74 ± 2.82	0.53
		0.25	28.80 ± 2.94	
		0.5	48.95 ± 2.85	
		1.0	66.23 ± 3.02	
		2.0	76.13 ± 2.97	
PUP80S1	812.65 ± 25.12	0.1	5.14 ± 2.02	0.93
		0.25	21.36 ± 2.75	
		0.5	38.37 ± 2.57	
		1.0	51.70 ± 2.84	
		2.0	57.21 ± 3.07	
Vc	–	0.1	72.31 ± 2.31	<0.1
		0.25	89.38 ± 2.34	
		0.5	95.62 ± 2.38	
		1.0	97.58 ± 2.29	
		2.0	97.89 ± 2.41	

[a] TE corresponds to Trolox.
[b] Data are expressed as mean ± SD.

frequency of branching (around 40.0%), more uronic acids and no β-(1→3)-D-Glc*p* in its backbone. Therefore, PUP80S1 represents a novel polysaccharide extracted from sclerotia of *P. umbellatus*.

3.4. Molecular morphology

AFM was used to directly observe its molecular morphology to obtain the chain conformation of PUP80S1. PUP80S1 was determined to exist in a sphere-like chain conformation in water based on the spherical particles observed in Fig. 4. A similar globular chain conformation was also reported for polysaccharides from other sources, like *Ganoderma lucidum* (Wang et al., 2011) and *Rhizoma Panacis Japonici* (Huang, Huang, Li, & Zhang, 2009; Huang, Ren, Duan, & Zhang, 2010). This conformation may be related to their branched structures (Huang et al., 2009).

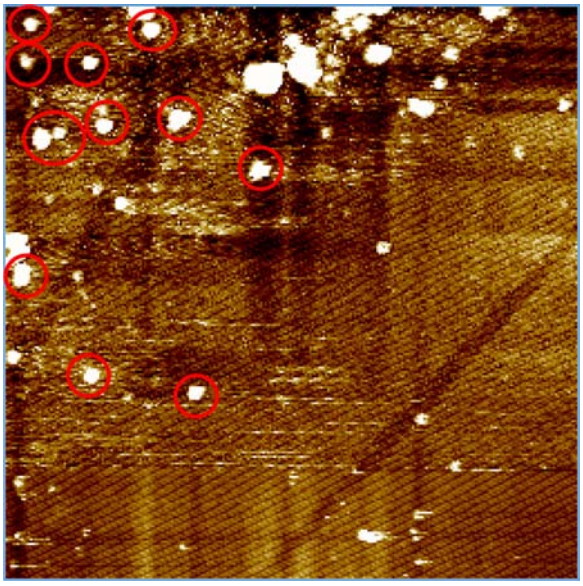

Fig. 4. Molecular Morphology of PUP80S1 revealed by AFM. Spherical particles, as highlighted by red marks, implied the spherical conformation. (For interpretation of the references to colour in this figure legend, the reader is referred to the web version of this article.)

3.5. Structure-activity relationship of polysaccharide

As described in section 3.3, PUP60S2 and PUP80S1 have similar structural properties. PUP60S2 has also a low molecular weight (14.4 kDa) and the same hexose residues as PUP80S1. Furthermore, PUP60S2 has also a backbone comprised of β-(1→6)-D-glucopyranosyl which is substituted at *O*-3 by side chains. But PUP60S2 possesses a greater frequency of branching (around 40.0%) and more uronic acids (22.3%). Given that these slight differences, we compared their antioxidant properties to gain a better understanding of their structure-activity relationship.

ORAC and DPPH assays were performed to investigate antioxidant activities. Both PUP80S1 and PUP60S2 exhibit good antioxidant capacities evident from their ORAC values of 812.65 ± 25.12 and 958.32 ± 26.05 μmol TE/g (Table 3), respectively, which were higher than those of polysaccharides from mung bean (Yao, Zhu, & Ren, 2016) and *Laminaria japonica* (Lu, You, Lin, Zhao, & Cui, 2013). DPPH assays revealed that PUP80S1 and PUP60S2 exhibit dose-dependent scavenging abilities for free radicals over the concentrations tested. They reach their maximum scavenging efficiency of (57.21 ± 3.07)% and (76.13 ± 2.97)% at 2.0 mg/mL, respectively, and have IC_{50} values of 0.93 and 0.53 mg/mL (Table 3). These results demonstrate that PUP80S1 and PUP60S2 both have excellent scavenging abilities against DPPH despite a somewhat lower efficiency than Vc, but PUP60S2 showed better scavenging abilities than PUP80S1. The better scavenging abilities of PUP60S2 than PUP80S1 were also found in hydroxyl and superoxide radicals scavenging tests (See Supplemental data).

Oxidative stress, induced by excess of reactive oxygen species, has been suggested to be the cause of aging and various chronic diseases in humans (Finkel & Holbrook, 2000; Halliwell, 2007). Hence, much attention has been paid to search for natural antioxidants against oxidative damage from occurring in the body. Excellent antioxidant abilities suggested that PUP80S1 and PUP60S2 could be potential antioxidants for use in food and nutraceuticals. While distinctive differences could be easily found between PUP80S1 and PUP60S2 from Table 3, which are possibly caused by their different structural features. Uronic acids are acknowledged as an important role in antioxidant activity. Polysaccharides containing higher content of uronic acids are found to show better antioxidant activities (Chen, Zhang, & Xie, 2004; Wu et al., 2014). Degree of branching is also reported to be related to antioxidant activities. Higher degree of branching is beneficial for exerting antioxidant activity for polysaccharide from *Schisandra sphenanthera* (Zhao et al., 2014).

Thus, the higher antioxidant activity of PUP60S2 may be ascribed to its higher levels of uronic acid and its higher degree of branching. Certainly, this structure-function relationship and its mechanism needs to be clarified in further studies.

4. Conclusion

A novel water-soluble polysaccharide, PUP80S1, was prepared from the sclerotia of *P. umbellatus* using a series of purification procedures. PUP80S1 exhibits a homogeneous molecular weight distribution with an average of 8.8 kDa in 0.1 M $NaNO_3$ solution and was determined to contain around 8.5% uronic acid. It was confirmed to be a branched polysaccharide with the unique primary structure shown in Fig. 3. AFM revealed that PUP80S1 exists in a sphere-like chain conformation in water. PUP80S1 is a novel polysaccharide different from those reported previously, including our previously reported PUP60S2 from the sclerotia of *P. umbellatus*. Although PUP80S1 and PUP60S2 possess similar low molecular weight, similar backbone and same hexose residues, lower levels of frequency of branching and uronic acids present in PUP80S1. Antioxidant tests reveal that PUP80S1 and PUP60S2 exhibit good antioxidant activity, but PUP60S2 show significantly higher antioxidant activities owing to its distinctly higher level of frequency of branching and uronic acids. The results presented suggest that the structural features have significant effects on functions of polysaccharides from the sclerotia of *P. umbellatus*. These findings promote our understanding of structure of polysaccharides from sclerotia of *P. umbellatus* and their structure-function relationships. The detailed mechanism of these activities still require further clarification.

Acknowledgements

The study was supported by Chinese Key Technology R&D Program of the twelfth Five-year Plan (No. 2013BAD16B07) and National Natural Science Foundation of China (No. 31571759).

Appendix A. Supplementary data

Supplementary data associated with this article can be found, in the online version, at http://dx.doi.org/10.1016/j.carbpol.2016.07.010.

References

Anumula, K. R., & Taylor, P. B. (1992). A comprehensive procedure for preparation of partially methylated alditol acetates from glycoprotein carbohydrates. *Analytical Biochemistry*, *203*(1), 101–108.

Bensky, D., Gamble, A., & Kaptchuk, T. J. (1993). . Chinese herbal medicine: materia medica.

Blumenkrantz, N., & Asboe-Hansen, G. (1973). New method for quantitative determination of uronic acids. *Analytical Biochemistry*, *54*(2), 484–489.

Chen, H., Zhang, M., & Xie, B. (2004). Quantification of uronic acids in tea polysaccharide conjugates and their antioxidant properties. *Journal of Agricultural and Food Chemistry*, *52*(11), 3333–3336.

Chen, L., Liu, J., Zhang, Y., Dai, B., An, Y., & Yu, L. L. (2015). Structural, thermal, and anti-inflammatory properties of a novel pectic polysaccharide from Alfalfa (*Medicago sativa* L.) stem. *Journal of Agricultural and Food Chemistry*, *63*(12), 3219–3228.

Dávalos, A., Gómez-Cordovés, C., & Bartolomé, B. (2004). Extending applicability of the oxygen radical absorbance capacity (ORAC-fluorescein) assay. *Journal of Agricultural and Food Chemistry*, *52*(1), 48–54.

Dai, H., Han, X.-Q., Gong, F.-Y., Dong, H.-L., Tu, P.-F., & Gao, X.-M. (2012). Structure elucidation and immunological function analysis of a novel beta-glucan from the fruit bodies of *Polyporus umbellatus* (Pers.) Fries. *Glycobiology*, *22*(12), 1673–1683.

Dubois, M., Gilles, K. A., Hamilton, J. K., Rebers, P. A., & Smith, F. (1956). Colorimetric method for determination of sugars and related substances. *Analytical Chemistry*, *28*(3), 350–356.

Ferreira, S. S., Passos, C. P., Madureira, P., Vilanova, M., & Coimbra, M. A. (2015). Structure-function relationships of immunostimulatory polysaccharides: a review. *Carbohydrate Polymers*, *132*, 378–396.

Filisetti-Cozzi, T. M., & Carpita, N. C. (1991). Measurement of uronic acids without interference from neutral sugars. *Analytical Biochemistry*, *197*(1), 157–162.

Finkel, T., & Holbrook, N. J. (2000). Oxidants, oxidative stress and the biology of ageing. *Nature*, *408*(6809), 239–247.

Forget, A., Christensen, J., Ludeke, S., Kohler, E., Tobias, S., Matloubi, M., et al. (2013). Polysaccharide hydrogels with tunable stiffness and provasculogenic properties via alpha-helix to beta-sheet switch in secondary structure. *Proceedings of the National Academy of Sciences of the United States of America*, *110*(32), 12887–12892.

Gheysen, K., Mihai, C., Conrath, K., & Martins, J. C. (2008). Rapid identification of common hexapyranose monosaccharide units by a simple TOCSY matching approach. *Chemistry: A European Journal*, *14*(29), 8869–8878.

Halliwell, B. (2007). Oxidative stress and cancer: have we moved forward? *Biochemical Journal*, *401*(1), 1–11.

Han, X.-Q., Chai, X.-Y., Jia, Y.-M., Han, C.-X., & Tu, P.-F. (2010). Structure elucidation and immunological activity of a novel polysaccharide from the fruit bodies of an edible mushroom, *Sarcodon aspratus* (Berk.) S. Ito. *International Journal of Biological Macromolecules*, *47*(3), 420–424.

He, P.-f., Zhang, A.-q., Wang, X.-l., Qu, L., Li, G.-l., Li, Y.-p., et al. (2016). Structure elucidation and antioxidant activity of a novel polysaccharide from Polyporus umbellatus sclerotia. *International Journal of Biological Macromolecules*, *82*, 411–417.

Hua, D., Zhang, D., Huang, B., Yi, P., & Yan, C. (2014). Structural characterization and DPPH• radical scavenging activity of a polysaccharide from Guara fruits. *Carbohydrate Polymers*, *103*(0), 143–147.

Huang, Z., Huang, Y., Li, X., & Zhang, L. (2009). Molecular mass and chain conformations of *Rhizoma Panacis Japonici* polysaccharides. *Carbohydrate Polymers*, *78*(3), 596–601.

Huang, Z., Ren, H., Duan, X., & Zhang, L. (2010). Chain conformation and bioactivity of water-soluble polysaccharide extracted from *Rhizoma Panacis Japonici*. *Biopolymers*, *93*(4), 383–390.

Jin, M., Zhao, K., Huang, Q., Xu, C., & Shang, P. (2012). Isolation, structure and bioactivities of the polysaccharides from *Angelica sinensis* (Oliv.) Diels: a review. *Carbohydrate Polymers*, *89*(3), 713–722.

Li, X., Xu, W., & Chen, J. (2010). Polysaccharide purified from *Polyporus umbellatus* (Per) Fr induces the activation and maturation of murine bone-derived dendritic cells via toll-like receptor 4. *Cellular Immunology*, *265*(1), 50–56.

Liao, S.-F., Liang, C.-H., Ho, M.-Y., Hsu, T.-L., Tsai, T.-I., Hsieh, Y. S.-Y., et al. (2013). Immunization of fucose-containing polysaccharides from Reishi mushroom induces antibodies to tumor-associated Globo H-series epitopes. *Proceedings of the National Academy of Sciences*, *110*(34), 13809–13814.

Lin, Y. F., & Wu, G. L. (1988). Protective effect of *Polyporus umbellatus* polysaccharides on toxic hepatitis in mice. *Acta Pharmacologica Sinica*, *9*(4), 345–348.

Liu, Y., Zhang, J., Tang, Q., Yang, Y., Guo, Q., Wang, Q., et al. (2014). Physicochemical characterization of a high molecular weight bioactive β-d-glucan from the fruiting bodies of *Ganoderma lucidum*. *Carbohydrate Polymers*, *101*, 968–974.

Lu, J., You, L., Lin, Z., Zhao, M., & Cui, C. (2013). The antioxidant capacity of polysaccharide from *Laminaria japonica* by citric acid extraction. *International Journal of Food Science & Technology*, *48*(7), 1352–1358.

Mizrahy, S., & Peer, D. (2012). Polysaccharides as building blocks for nanotherapeutics. *Chemical Society Reviews*, *41*(7), 2623–2640.

Nejatzadeh-Barandozi, F., & Enferadi, S. T. (2012). FT-IR study of the polysaccharides isolated from the skin juice, gel juice, and flower of *Aloe vera* tissues affected by fertilizer treatment. *Organic and Medicinal Chemistry Letters*, *2*(33), 1–9.

Nie, S., Zhang, H., Li, W., & Xie, M. (2013). Current development of polysaccharides from *Ganoderma*: Isolation, structure and bioactivities. *Bioactive Carbohydrates and Dietary Fibre*, *1*(1), 10–20.

Peng, K., Lan, L. S., Yan, W. X., Jie, S. L., Wu, Y. J., Hua, Z. Y., et al. (2012). *Polyporus umbellatus* polysaccharides ameliorates carbon tetrachloride-induced hepatic injury in mice. *Afr. J. Pharm. Pharmacol*, *6*, 2686–2691.

Perez-Mendoza, D., Rodriguez-Carvajal, M. A., Romero-Jimenez, L., Farias Gde, A., Lloret, J., Gallegos, M. T., et al. (2015). Novel mixed-linkage beta-glucan activated by c-di-GMP in Sinorhizobium meliloti. *Proceedings of the National Academy of Sciences of the United States of America*, *112*(7), E757–765.

Prajapati, V. D., Maheriya, P. M., Jani, G. K., & Solanki, H. K. (2014). Carrageenan: a natural seaweed polysaccharide and its applications. *Carbohydrate Polymers*, *105*, 97–112.

Ruiz-Matute, A. I., Hernández-Hernández, O., Rodríguez-Sánchez, S., Sanz, M. L., & Martínez-Castro, I. (2011). Derivatization of carbohydrates for GC and GC–MS analyses. *Journal of Chromatography B*, *879*(17–18), 1226–1240.

Ruthes, A. C., Smiderle, F. R., & Iacomini, M. (2016). Mushroom heteropolysaccharides: a review on their sources: structure and biological effects. *Carbohydrate Polymers*, *136*, 358–375.

Taylor, R. L., & Conrad, H. E. (1972). Stoichiometric depolymerization of polyuronides and glycosaminoglycuronans to monosaccharides following reduction of their carbodiimide-activated carboxyl groups. *Biochemistry*, *11*, 1383–1388.

Ueno, Y., Abe, M., Yamauchi, R., & Kato, K. (1980). Structural analysis of the alkali-soluble polysaccharide from the sclerotia of *Grifora umbellata* (Fr.) Pilat. *Carbohydrate Research*, *87*(2), 257–264.

Ueno, Y., Okamoto, Y., Yamauchi, R., & Kato, K. (1982). An antitumor activity of the alkali-soluble polysaccharide (and its derivatives) obtained from the sclerotia of *Grifora umbellata* (Fr.) Pilát. *Carbohydrate Research*, *101*(1), 160–167.

Venkatesan, J., Qian, Z.-J., Ryu, B., Ashok Kumar, N., & Kim, S.-K. (2011). Preparation and characterization of carbon nanotube-grafted-chitosan -natural hydroxyapatite composite for bone tissue engineering. *Carbohydrate Polymers*, *83*(2), 569–577.

Wang, J., Ma, Z., Zhang, L., Fang, Y., Jiang, F., & Phillips, G. O. (2011). Structure and chain conformation of water-soluble heteropolysaccharides from *Ganoderma lucidum*. *Carbohydrate Polymers*, *86*(2), 844–851.

Wolfrom, M. L., & Thompson, A. (1963a). Acetylation. In R. L. Whistler, & M. L. Wolfrom (Eds.), *Methods in carbohydrate chemistry* (Vol. 2) (pp. 211–215). New York: Academic Press.

Wolfrom, M. L., & Thompson, A. (1963b). Reduction with sodium borohydride. In R. L. Whistler, & M. L. Wolfrom (Eds.), *Methods in carbohydrate chemistry* (Vol. 2) (pp. 65–67). New York: Academic Press.

Wu, H., Liang, J., Cheng, Y., Huang, H., Wu, K., & Chiang, S. (2011). Radio- and chemoprotective effects of Zhu-Ling Mushroom *(Polyporus umbellatus)* in human cultured cells and in mice. *Toxicology Letters*, *205* [S37–S37

Wu, S., Li, F., Jia, S., Ren, H., Gong, G., Wang, Y., et al. (2014). Drying effects on the antioxidant properties of polysaccharides obtained from *Agaricus blazei Murrill*. *Carbohydrate Polymers*, *103*, 414–417.

Yao, Y., Zhu, Y., & Ren, G. (2016). Antioxidant and immunoregulatory activity of alkali-extractable polysaccharides from mung bean. *International Journal of Biological Macromolecules*, *84*, 289–294.

Yin, J.-Y., Lin, H.-X., Nie, S.-P., Cui, S. W., & Xie, M.-Y. (2012). Methylation and 2D NMR analysis of arabinoxylan from the seeds of *Plantago asiatica* L. *Carbohydrate Polymers*, *88*(4), 1395–1401.

Zhang, G., Zeng, X., Li, C., Li, J., Huang, Y., Han, L., et al. (2011). Inhibition of urinary bladder carcinogenesis by aqueous extract of sclerotia of *Polyporus umbellatus* fries and polyporus polysaccharide. *American Journal of Chinese Medicine*, *39*(1), 135–144.

Zhang, Z., Wang, F., Wang, M., Ma, L., Ye, H., & Zeng, X. (2015). A comparative study of the neutral and acidic polysaccharides from *Allium macrostemon* Bunge. *Carbohydrate Polymers*, *117*, 980–987.

Zhao, T., Mao, G., Feng, W., Mao, R., Gu, X., Li, T., et al. (2014). Isolation: characterization and antioxidant activity of polysaccharide from *Schisandra sphenanthera*. *Carbohydrate Polymers*, *105*, 26–33.